Journal of Molecular Liquids 210 (2015) 2–8

Contents lists available at ScienceDirect

Journal of Molecular Liquids

journal homepage: www.elsevier.com/locate/molliq

# The study of nanostructured liquids by cryogenic-temperature electron microscopy — A status report

Yeshayahu Talmon

*Department of Chemical Engineering and the Russell Berrie Nanotechnology Institute (RBNI), Technion — Israel Institute of Technology, Haifa 32000, Israel*

ARTICLE INFO

Available online 29 April 2015

*Keywords:*
Cryo-TEM
cryo-SEM
Complex liquids
Nanostructure
Microemulsions
Lyotropic liquid crystals

ABSTRACT

Cryogenic-temperature transmission electron microscopy (cryo-TEM) is now a standard tool in the study of complex liquids, i.e., liquid systems with aggregates or building blocks on the nanometric scale. Methodologies have been developed to help capture the nanostructure of liquid systems, while preserving their original state at a given concentration and temperature. Cryo-TEM is now widely used to study synthetic, biological, and medical systems. Originally developed for aqueous systems, it has been also applied successfully in the study of non-aqueous systems, even in unusual solvents, such as strong acids. Recent developments in high-resolution scanning electron microscopy (HR-SEM) have made it an ideal tool for the study of nanoparticles and colloids in viscous systems or in systems containing large objects, three hundred nanometers and larger, in which small (nanometric) features are to be imaged, e.g., hydrogels or biological cells. Such system cannot be studied by cryo-TEM. Liquid nanostructured systems can now be studied by cryogenic-temperature scanning electron microscopy (cryo-SEM), using much-improved cryogenic specimen holders and transfer systems, even without conductive coating. In recent years we have developed a novel specimen preparation methodology for cryo-SEM specimens that preserves the original nanostructure of labile complex liquids at specified composition and temperature, quite similarly to what has been done in cryo-TEM. Here I describe briefly the state-of-the-technology of cryo-TEM and cryo-SEM, and demonstrate various variants of the methodology that allow the study of a wide range of nanostructured (soft matter) systems, taking advantage also of the combination of cryo-TEM and cryo-SEM.



## 1. Introduction

Quite often the tool of choice for high-resolution direct imaging of any material system is an electron microscope (EM), either a transmission electron microscope (TEM), or a scanning electron microscope (SEM). To image with an EM a specimen containing highly volatile components, such as water or many oils, steps should be taken to make the specimen compatible with the high vacuum in the EM, a process called 'fixation'. Chemical fixation, such as staining with a salt or an acid of a heavy metal, followed by drying the specimen, may be used only if the specimen is stable enough to undergo such harsh treatment, while preserving its nanostructure. The fixation method of choice is not chemical, but physical, i.e., fast cooling of the liquid, high-vapor-pressure specimen to cryogenic temperatures, at which it does not flow, and its vapor pressure is much lower than the pressure in the EM column, namely, less than $10^{-6}$ mbar ($10^{-4}$ Pa). Ideally the liquid components should not freeze, but vitrify, i.e., become a very high-viscosity, low-vapor-pressure material, namely, a glass. Cryogenic electron microscopy was originally developed by biologists or biophysicists, who attempted to examine biological system at conditions as close as possible to their native state. Among the pioneers in that area were Patrick Echlin, who developed an early methodology of cryogenic-temperature SEM (cryo-SEM) [1], and Robert Glaeser, who worked on cryogenic-temperature TEM (cryo-TEM) [2]. An important breakthrough was the demonstration of successful vitrification (as opposed to freezing) of cryo-TEM specimen by Jacques Dubochet and his colleagues [3]. As commercial manufacturers introduced cryo-specimen holders, it gradually became easier to perform cryo-TEM. Cryo-SEM took the same path, but has never been as widely used as cryo-TEM.

Fairly early in the development of cryo-EM, it became apparent that the presence of water in the specimen, in the form of ice, either crystalline or vitreous (supercooled water), enhances electron-beam radiation-damage considerably, making imaging of those specimens quite problematic [4]. It has turned out that the very rapid free-radical reaction that follows irradiation of a cryo-EM specimen with an electron beam takes place at the interface between organic matter and water [5]. When water is mixed with organics, e.g., sucrose, radiation damage becomes very rapid. Before long it became apparent that to collect high-resolution data from cryo-EM specimens one needs to expose the specimen to no more than about 10 $e^{-}/Å^2$, which is $10^4$ to $10^5$ less electrons than most electron microscopy specimens experience before an image is recorded.

Many of the biological cryo-EM specimens are fairly stable with respect to temperature and concentration changes (within a certain

http://dx.doi.org/10.1016/j.molliq.2015.03.054
0167-7322/

range). Of course, all biological systems are water-based systems. The situation is different with more general specimens in the realm of physical chemistry. While water-based systems are very important in that area, many are complex systems of several components, including water, which form a spectrum of nanostructures, very sensitive to concentration and temperature changes. It is obvious that the nanostructure of such systems cannot be preserved when an alien compound (a stain or a fixative) is added. Obviously, fast cooling is the preferred method of preparation for such systems. To ascertain that the nanostructure in the vitrified specimen reflects that of the bulk system, preparation of the cryo-TEM or cryo-SEM specimen has to be carried out in an environment where temperature is fixed at a desired value, and evaporation of the volatiles from the specimen is prevented by proper saturation of the atmosphere around the prepared specimen. This calls for a proper sample preparation chamber. The first successful one was the 'Controlled Environment Vitrification System' (CEVS), designed and introduced by Bellare et al. [6]; it is still in use in various versions and modifications in many laboratories worldwide. Commercial apparatuses based on the same general idea, but designed for automated specimen preparation are now available. The CEVS was originally developed for the preparation of thin cryo-TEM specimens, as are the commercial units.

While cryo-TEM is now a well-established methodology that can be applied in the study of a wide range of biological and synthetic systems, quite often it needs to be replaced or augmented by cryo-SEM. This is the case when the liquid system to be studied is either very viscous, and thus cannot be made into the thin liquid films that are vitrified into a cryo-TEM specimen, or when the system contains objects that are too large to fit in the thin cryo-TEM specimen, typically less than 300 nm thick, but where we look for nanometric details. SEM cryo-holders are also available from a number of manufacturers. The need for specimen preparation under controlled conditions exists, of course, also in the case of cryo-SEM. This need has been answered a couple of years ago by Issman and Talmon [7] who modified the CEVS to accommodate cryo-SEM specimen preparation under controlled temperature and surrounding air saturation. The same apparatus may be used also for the preparation of freeze-fracture replicas under controlled conditions [8].

When systems that are either entirely composed of non-aqueous components, or those where the continuous phase is non-aqueous, are to be examined by cryo-EM, special precautions must be taken. Many organics are either flammable, or their vapors form explosive mixtures with air, thus the CEVS should be placed in an efficient fume-hood. Note that the commercial systems mentioned above can be used only for specimen preparation of aqueous systems. For non-aqueous systems the cryogen of choice, liquid ethane at its freezing point, i.e., "liquid–solid ethane", LSE, cannot be used, as it is a good solvent for most organic liquids. Instead we use boiling liquid nitrogen, $LN_2$, a far less efficient coolant. However, the relatively low cooling rates achievable by $LN_2$, no more than 8000 K/s (as compared to 100,000 provided by LSE), are sufficient to vitrify most organic solvents, except for linear hydrocarbons [9]. In recent years we have extended cryo-EM of nonaqueous systems even to the extreme of systems based on superacids, such as oleum and chlorosulfonic acid (CSA) [10]. In that case water and any organic material should not come in contact with CSA, as water causes it to disintegrate into hydrochloric and sulfuric acids, and it oxidizes easily any organic material. Thus, when working with CSA the CEVS is continuously flushed with dry nitrogen gas, and blotting of the specimen, a necessary step in cryo-EM preparation is done with fiberglass, not paper, sheets. Fast cooling is achieved by plunging the specimen into $LN_2$, not LSE, which gives sufficient cooling rates to vitrify CSA [11].

The above paragraphs describe the main cryo-EM tools that are available nowadays for the study of liquid systems that contain nanostructures or aggregates of a few to a several hundred nanometers, quite often called 'complex liquids' or 'nanostructured liquids'. Many of those liquid systems are related to biology and medicine, many others are synthetic. Some are water-based, some are water-free, and others are made of both oil and water. Quite often those systems have important technical and economical applications. The nanostructure of such systems depends on the molecular structure of their components, and has a profound effect on their macroscopic properties. Direct imaging of complex liquids is essential to determine the building blocks of those systems. In some cases one could use both cryo-TEM and cryo-SEM on the same system. Agreement between the images obtained by the two methodologies may rule out specimen preparation and imaging artifacts. Sometimes, if larger objects are present, or when in a process, smaller aggregates evolve into larger ones, light microscopy, especially using differential interference contrast (Nomarski) optics, or polarized light between crossed polarizers, can also augment the EM data. Whenever possible, imaging should be complemented by other experimental techniques, such as X-ray or neutron scattering, NMR, or electrical conductivity measurements. Those could support suggested models based on imaging, and give accurate measurements to the suggested nanostructure.

Following this introduction I will survey several relatively recent applications of cryo-EM in the study of a number of diverse complex liquids. My aim is to demonstrate the strength of the methodology and the breadth of its application. I would also like to demonstrate how the methodology is fine-tuned to accommodate the specific nature of each studied system.

## 2. Microemulsions

The original incentive to develop cryo-EM was the study of biological systems, all of which contain water. Water is also present in many other systems of interest. And water has turned out to be a relatively easy substance to work with, as it is safe, it can be vitrified in SLE, and vitrified water gives reasonably good contrast relative to the aggregates that biological systems contain. It is true that water is easily radiolyzed by the electron beam, producing free radicals that attack organic material in the irradiated areas of the specimen, but using low-dose imaging techniques, one can record good images of such specimens with minimal damage. Extending cryo-EM (originally cryo-TEM only, and more recently cryo-SEM) to non-aqueous systems turned out to be quite challenging. Fortunately it is quite easy to vitrify organic solvents in liquid nitrogen (except for normal hydrocarbons), but it has been found out that those specimen are typically more electron beam sensitive than aqueous ones, although careful low-dose imaging does work for most specimens, with the one notable exception of DMSO (dimethylsulfoxide; Talmon, unpublished results). However, quite often contrast between the imaged aggregates and the organic solvent is rather low, and may be enhanced by electron beam selective etching in cryo-TEM [12], or by selective sublimation in cryo-SEM [13].

In my own research an on-going theme has been the study of microemulsions (MEs). While water continuous microemulsions, namely aqueous systems of oil-swollen micelles, can be imaged just like any other aqueous system [14], oil continuous or bicontinuous MEs pose a much more difficult challenge for cryo-EM. In addition, many MEs are very sensitive to relatively small changes of concentration and temperature, and thus much care should be taken during specimen preparation to keep those parameters constant at all times, until the specimen is vitrified. Quite often we study a system over a wide range of concentrations and temperatures. In that case a combination of cryo-TEM and cryo-SEM should be used. In some cases both methodologies can be used for a given system, and thus mutually support the validity of the results obtained by each. In other cases only one of those methodologies can be used in a given part of the phase diagram due to considerations of specimen preparation or imaging.

A good example of the application cryo-SEM to study a bicontinuous or an oil-continuous microemulsion is the study of ternary DDAB-water-octane microemulsions originally studied quite some time ago by Ninham, Evans and their coworkers [15]. Fig. 1a shows a cryo-SEM

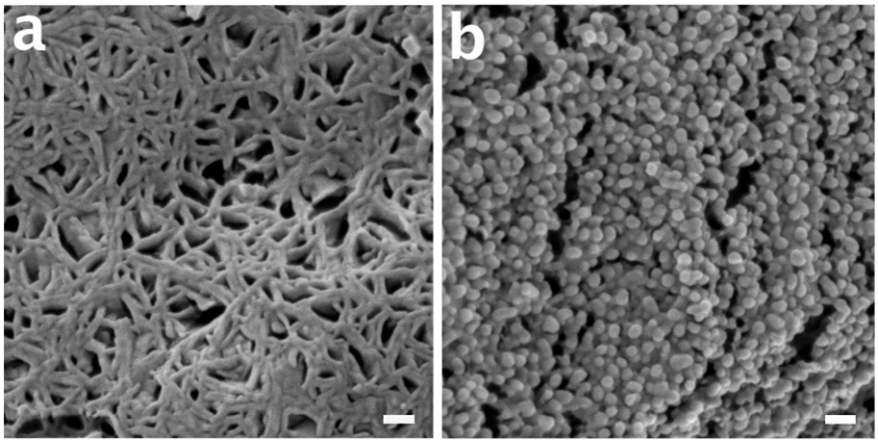


**Fig. 1.** a. Cryo-SEM of 48%/32%/20 wt.% isooctane/DDAB/water microemulsion; b. 36%/24%/40 wt.% isooctane/DDAB/water microemulsion. Bars = 100 nm. From [13].

micrograph of a 48%/32%/20 wt.% isooctane/DDAB/water system. In this case we replaced the octane in the original study by isooctane, as the latter can be vitrified in liquid nitrogen, while the former cannot. Such change introduces only minor changes in the phase diagram, as we found experimentally. The network structure we observe is the nanostructure was predicted by the original authors for low water content microemulsions. The lighter network seen is made of inverse water-swollen threadlike (cylindrical) micelles, about 20–30 nm in diameter. In fact, this structure is very similar to the model cartoon suggested over 25 years earlier by Chen et al. [16]. The excellent image contrast in the cryo-SEM micrograph is the result of the sublimation of the isooctane during handling of the cryo-specimen, because of the appreciable vapor pressure of isooctane at cryogenic temperature, while the vapor pressure of water is negligible at those conditions [13].

In a more water-rich microemulsion of 36%/24%/40 wt.% isooctane/DDAB/water we observed spherical and slightly elongated inverse water-swollen micelles, about 30–50 nm in diameter (Fig. 1b). Again, the micrographs agree with the previous studies of Ninham, Evans, and their colleagues. Such direct imaging supports the original theoretical model that explained why at low water content the system is electrical conductive (water is continuous, as we have shown), while at higher water content the electrical conductivity is very low, because the water is now in isolated domains, although it is the major component of the system. We have shown this type of nanostructure in another microemulsion system, and have termed this type of structure 'high internal phase microemulsion' ("HIPME") [17].

We have also studied microemulsion systems containing water, oil, and a nonionic surfactant. Such systems had been extensively studied in the 1980s by Kahlweit and his colleagues [18], but had never been directly imaged, although, as mentioned above, those MEs had been studied by freeze-fracture-replication by Strey and Jahn [19]. In our on-going work we have used both cryo-TEM and cryo-SEM to directly image MEs containing different ratios of water/isooctane at a constant concentration (7 wt.%) of the non-ionic surfactant $C_{12}E_5$. We have followed the nanostructural changes as we changed the oil-to-oil + water ("oil-to-solution") ratio in the system, and the temperature, staying in the monophasic regime of the phase diagram, as reported by Kahlweit et al. [18]. As in the previous example we have used the branched isooctane instead of the original n-octane, since the former can be vitrified even in $LN_2$.

Fig. 2 shows cryo-EM images of two samples, one has an oil-to-solution ratio, $\alpha = 30$ wt.%., and the other has an oil-to-solution ratio, $\alpha = 80$ wt.%; they were quenched into $LN_2$ at temperatures of 31 °C and 37 °C, respectively. The CEVS was saturated by the MEs themselves. As stated above, because of the high vapor pressure of isooctane at cryogenic temperatures, some of it was sublimed away during specimen manipulation, giving good contrast. Fig. 2a and 2b show cryo-TEM and cryo-SEM micrographs of the bicontinuous ME. The cryo-TEM image (Fig. 2a) is a projection of the sponge-like structure on the 2-D detector, while the cryo-SEM picture (Fig. 2b) shows very clearly the fractured surface of the thermally fixed sample after some isooctane has sublimed away, leaving behind the solid water domains.

Fig. 2c and 2d show cryo-TEM and cryo-SEM micrographs of the water-in-oil ME. In the cryo-TEM image (Fig. 2c) we see frozen (crystalline) water domains in the vitreous isooctane. The crystalline domains that are aligned with respect to the electron beam such that they satisfy Bragg's law, diffract electrons, and appear dark, while the others appear light. Defects in the ice domains are also apparent. The same water domains are seen in the cryo-SEM pictures (Fig. 2d) as light objects, typical of small objects on the surface of the specimen, following isooctane sublimation. A comprehensive report of this work is to be submitted for publication in the near future.

## 3. Liquid crystalline phases

An important class of nanostructured liquid phases is lyotropic liquid crystals that are found in numerous surfactant–water or surfactant–water-oil systems. Some of those were studied by cryo-TEM a long time ago [20]. In that study direct-imaging cryo-TEM was augmented by freeze-fracture-replication, when the system was too viscous. Full characterization was achieved by combining the microscopy data with small-angle X-ray scattering (SAXS), which identified the cubic liquid crystalline phase suggested by EM, as belonging to the rather rare space group, Pm3n.

The advent of the newly developed methodology of cryo-SEM mentioned above has allowed us to combine it with cryo-TEM, and sometimes with freeze-fracture-replication to achieve full nanostructural characterization of liquid crystalline phases. The first example of the application of the combination of the three EM techniques was shown by Omer et al. [21], who studied the formation of silica mesoporous materials, with a hexagonal and cubic-bicontinuous liquid crystalline phase as intermediates.

More recently the combination of state-of-the-art cryo-TEM and cryo-SEM has been used for mapping part so the phase diagram of water–lecithin–isooctane [22], a system that has been studied extensively over the years. Imaging was augmented by SAXS for a complete nanostructural analysis of the formed phases. The phase diagram shows various inverse micellar and liquid crystalline phases. We used cryo-TEM to image the nanostructures at the water-rich side of the phase-diagram. At higher lecithin and isooctane concentrations, cryo-SEM (Fig. 3a) reveals an ordered liquid crystalline phase made of small globular micelles. The inset shows the center area of the main image at higher magnification. While the apparent order has six-fold symmetry, this cross-section is insufficient to make a definitive

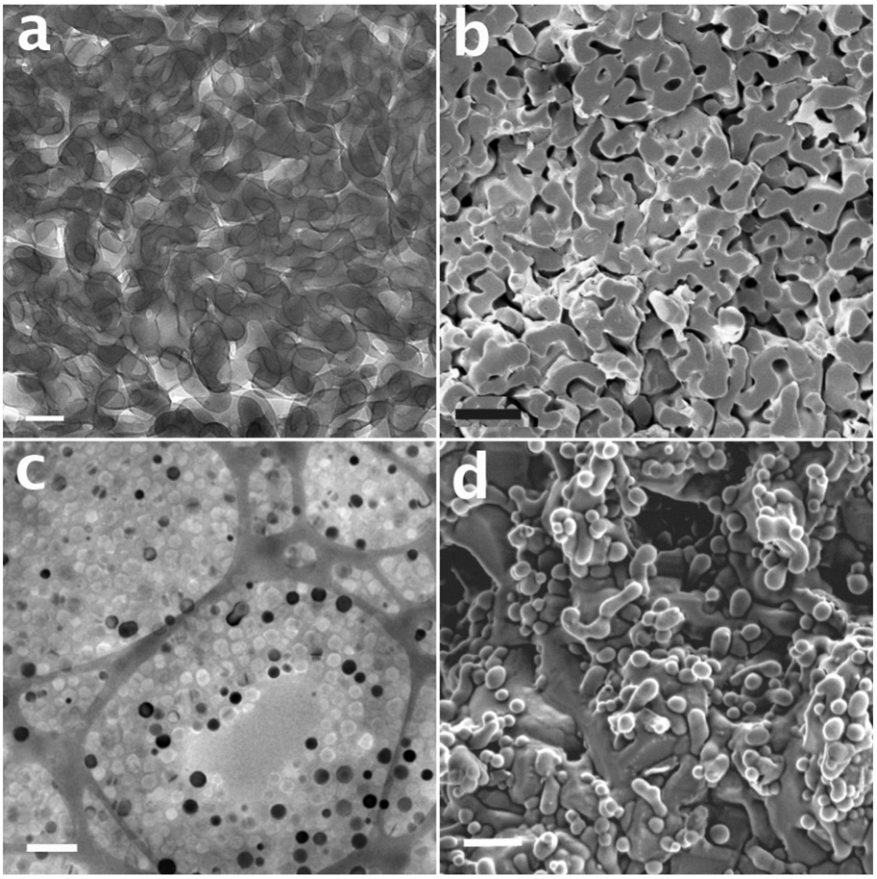


**Fig. 2.** Cryo-TEM (a & c) and cryo-SEM (b & d) of water–isooctane–$C_{12}E_5$ microemulsions, containing 7 wt.% of the nonionic surfactant. For a & b $\alpha = 40\%$.; samples were quenched from 34 °C. For c & d $\alpha = 80\%$; samples were quenched from 37 °C. Bars = 100 nm (a), 1 μm (b); 500 nm (c) and (d).

identification of this ordered liquid phase. In the same field of view we notice also larger globular structures, which correspond to another phase, coexisting with the former. Those could be liposomes of a lamellar phase. For full identification of the phases we used SAXS. Fig. 3b shows the spectrum obtained from the same system. The marked peaks suggest a cubic liquid crystalline phase of the Fd3m symmetry. The graph in Fig. 3c is a plot of the reciprocal d-spacings of the reflections marked in (b). The straight line connecting all the points corresponding to the peaks of the spectrum, and going through the origin, proves that the suggested symmetry agrees with the scattering data. The remaining peak corresponds to the lamellar phase of the liposomes.

## 4. "Extreme cryo-EM"

Probably the least suitable liquids to be studied by cryo-EM are strong acids. However, quite often strong acids are used as solvents in industrial applications. For example, chlorosulfonic acid (CSA) is the only practical solvent for carbon nanotubes (CNTs) [10]. To spin high-quality fibers from CNTs they should be first dissolved in a proper solvent, CSA in this case, to form a nematic liquid crystalline phase that is pushed through a spinneret into a liquid bath, where the acid disintegrates, leaving behind solid fibers, which are dried and spooled [23]. We have developed a new methodology based on cryo-TEM and cryo-SEM to allow us to study the nanostructure of CNTs in CSA solutions, from very dilute homogeneous solutions to the nematic liquid crystalline phase [11]. The methodology allows us to prepare cryo-EM specimens without harming the operator or the instruments, while preserving the original nanostructures in the strong acid. Instead of preparing the cryo-EM specimens in an atmosphere saturated with the liquid phase vapors, we have to work under inert, completely dry gas, because CSA forms HCl and $H_2SO_4$, upon contact with water molecules, as in humid air. Blotting is performed with fiberglass filter paper, because CSA oxidizes any organic substance it contacts. The specimens are quenched in $LN_2$ for the same reason. Fortunately $LN_2$ provides sufficient cooling rates to vitrify CSA. The vapor pressure of CSA is very low, thus evaporation during specimen preparation, or sublimation from the cryo-specimen is negligible. The same cryo-EM methodology has been used to study graphene, which can be also be dissolved in CSA [24]

Fig. 4a & 4b show cryo-TEM images of vitrified CNTs in CSA. Note that the contrast is "inverse", namely, the vitrified solvent appears quite dark, because it contains the relatively heavy atoms Cl and S, whereas the CNTs are pure carbon. In fact, in most such specimens it is very difficult to see the CNTs due to their very low contrast relative to the vitrified acid. That we see the CNTs quite well is due to selective etching of the acid at the acid-CNT interface. This process of electron-beam radiation-damage causes some acid loss very close to the CNTs (note lighter domains parallel to the CNTs), giving reasonably good contrast. We had used this phenomenon of selective etching before to enhance contrast between liposomes and a water–glycerol mixed solvent [12]. In that case radiation–damage rates were much higher at the water-organic matter interface, a phenomenon we had observed and explained years earlier [5]. Fig. 4a shows a very low AC299 CNT concentration of 20 ppm, giving almost a completely random dispersion of the CNTs in the acid. At the higher concentration of 200 ppm (Fig. 4b) we observe the beginning of ordering into bundles, which at more concentrated solution leads to formation of the nematic phase. That order is essential to preserve the excellent mechanical and electrical properties of a single CNT in the spun fibers.

At higher CNT concentration the system becomes rather viscous due to the formation of the nematic phase. The high viscosity prevents the preparation of the thin liquid films needed for cryo-TEM specimens,

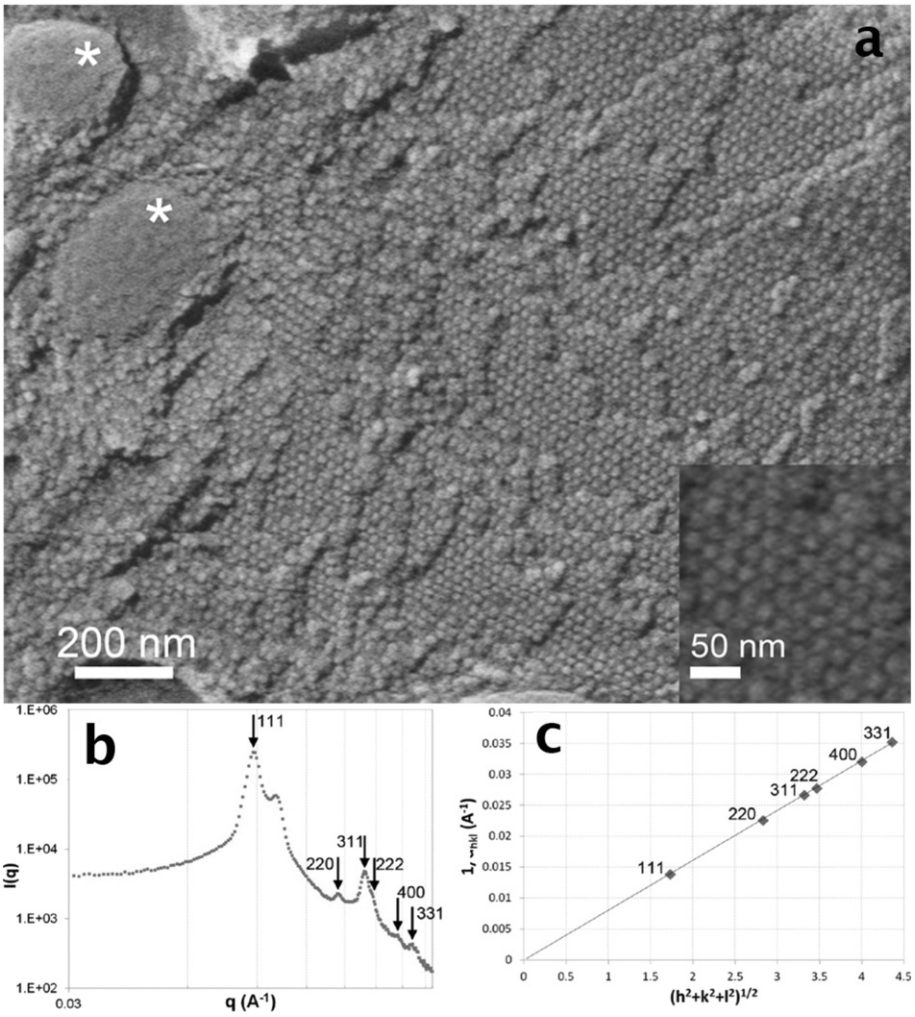


**Fig. 3.** 60/32.8/7.2 wt.% lecithin, isooctane and water at 25 °C. (a) Cryo-SEM picture showing an ordered phase (magnified in the inset), and larger globular objects (asterisks). b. SAXS spectrum of the system with arrows marking the positions of the Fd3m space-group. (c) Plot of the reciprocal d-spacings of the reflections marked in (b). From [22].

and thus we use cryo-SEM instead. Fig. 4c is a cryo-SEM micrograph of 0.7% dispersion of HiPco CNTs in CSA, giving an isotropic solution due to the rather short length of those specific CNTs. Fig. 4d shows the very well ordered nematic phase formed by 3% of the much longer CCNI1101 CNTs. The higher aspect ratio of the CCNI1101 CNTs and the higher concentration of the dispersion, both promote the observed order [25]. The insets in Fig. 4c & d are from the latter reference, Flory's classic paper of 1956 dealing with rigid-rod polymers, showing schematically the expected phases. By combining cryo-TEM and cryo-SEM we were able to map the entire range of nanostructures in this system, in the concentration range applicable for fiber spinning.

## 5. Other applications of cryo-TEM and cryo-SEM

In addition to what is described above, there are, of course, many more recent examples that show the power of combining cryo-EM techniques. Quite often one uses different specimen preparation techniques and different imaging conditions. For example, quite often there is a need to study by cryo-SEM the surface of a specimen, as is the case of a block copolymer isoporous membrane cast on a glass slide from a solution in mixed solvents. The selective evaporation of the solvents due to their very different vapor pressures causes nanostructural changes in the drying membrane, producing eventually the desired membrane. The process can be followed by repeating the cryo-SEM experiment several times, increasing the time from casting to vitrification for each experiment, thus performing in effect time-resolved cryo-SEM [26]. In the same system of the polystyrene-b-poly(4-vinylpyridine) (PS-b-P4VP) diblock copolymer cryo-TEM was also used to understand phase separation of the two types of polymer blocks in different solvents. Controlled electron-beam radiation damage was applied to generate contrast between the PS-rich and the P4VP-rich domains formed by phase separation, taking advantage of the faster mass loss due to radiolysis by the P4VP domains. That phase separation is needed for membrane formation.

The issue of contrast, or most often lack of sufficient contrast, is a recurring problem in cryo-EM of soft matter. Of course we normally avoid the use of adding any stains to the studied system, as those molecules may change the nanostructure we image [27]. Sometimes, however one can replace one type of molecule in the system by a similar one that contains a heavier atom that gives good contrast. We did it quite some time ago by replacing NaCl with CsCl in salt containing system, and indeed the heavier cation did give much better contrast, without changing the nanostructure of the system, molecules of poly(styrene sulfonate acid) grafted onto polystyrene spheres [28]. In a more recent study we used an iodine containing oil, Lipiodol, to follow by cryo-TEM the uptake path of the nanocapsules of a drug administered, either intravenously or orally, following their embedding in the gastro-resistant microparticles fed to mice [29].

The issue of contrast is encountered whenever we work with systems composed of molecules made almost solely of hydrogen, carbon and oxygen. Molecular groups that contain heavier atoms such as sulfates or phosphates do help, but quite often they are present in

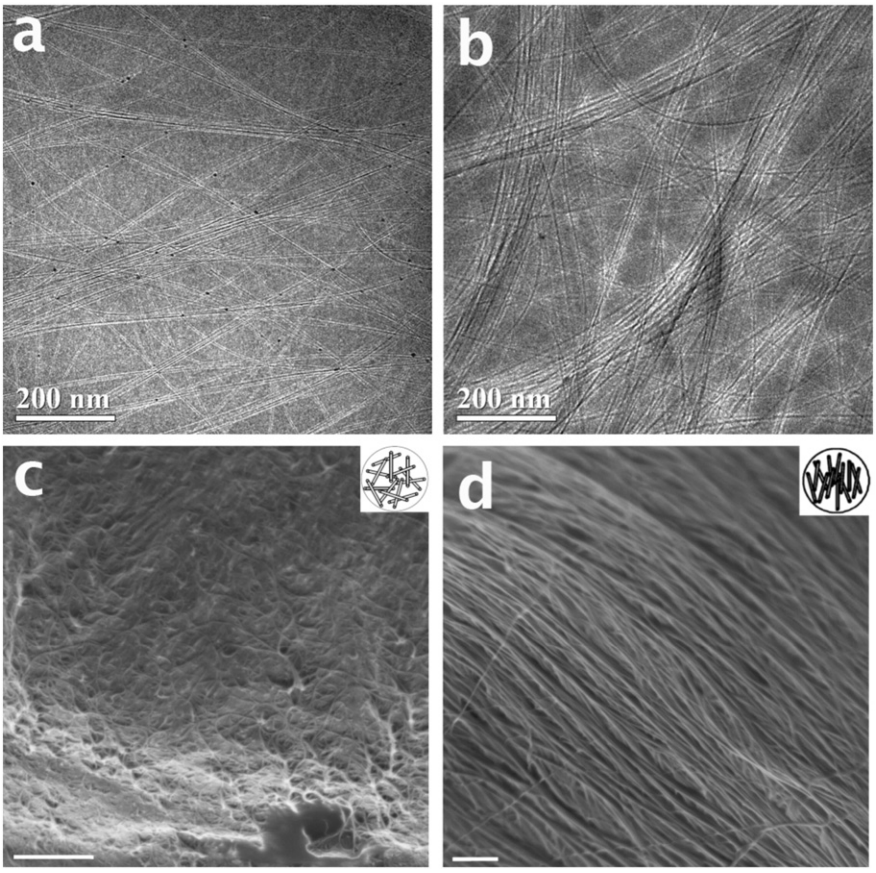


**Fig. 4.** Cryo-TEM (a & b) and cryo-SEM (c & d) micrographs of carbon nanotubes in chlorosulfonic acid. (a) 20 ppm AC299 CNTS; (b) 200 ppm AC299 CNTs; (c) 0.7 wt.% of HiPco CNTs giving an isotropic phase; (d) 3 wt.% of CCNI CNTs forming a well-ordered nematic phase. (c) and (d) are from [11]; bars = 500 nm.

two different chemical species, such as two different phospholipids. To distinguish between such molecules one could use tagging by gold nanoparticles attached to ligands that selectively attach to a certain group found on the surface of an aggregate, such as a biological cell, or a liposome. This is not a new concept, but so far it has been performed on dry specimens only, and thus is not applicable to many of the systems whose nanostructure is sensitive to changes of concentration and temperature. Only very recently there has been a report on an attempt to perform immunogold labeling in the liquid phase [30]. However the selectivity of the labeling could use improvement. Our group is actively working on finding a way to selectively label certain proteins or lipids that are found in mixed lipid liposomes, or in "microparticles" (which are really nanoparticles) and exosomes that are found normally in the blood, and at elevated concentration in pregnancy and in pathological conditions [31].

## 6. Conclusions

We have shown here the application of state-of-the-technology combination of cryo-TEM and cryo-SEM in the study of a wide range of liquid nanostructured systems. The present technology may be fine-tuned to study many other systems, aqueous or non-aqueous, synthetic, or biological. While the methodologies are quite versatile, one has to be familiar with their limitations, and whether and how they can be overcome. That calls for very good understanding the physics (and sometimes the chemistry) of specimen preparation, electron beam–specimen interaction, and image (TEM) or picture (SEM) formation. The possibility of artifact formation is ever present. Artifacts may be formed during specimen preparation and transfer into the microscope, and during imaging, as a result of electron-beam damage and image or picture formation. Cryo-EM specimens are especially prone to beam damage and to contaminant condensation from the microscope vacuum.

The best approach to the application of cryo-EM is to combine several microscopy techniques, such as cryo-TEM and cryo-SEM, or cryo-EM and light microscopy, whenever applicable. In addition, to obtain full and quantitative nanostructural characterization of complex liquid, one should use microscopy with non-imaging techniques, such as a scattering techniques, NMR, and measurement of rheological or electrical properties of the system. When microscopy and scattering techniques are combined, the former, if used properly and carefully, gives images of the building blocks of the system. Those may be used to form a physical model of the nanostructures, with which the scattering curves can be properly analyzed to give numerical measures of those building blocks. Examples to this approach are given in references [11, 17,21,22]. Disagreement between any of the techniques may point to experiment artifacts. Some of the most common cryo-TEM artifacts were discussed in a review by Talmon [32].

Cryo-EM has become widely used, and in many cases has replaced methodologies that are inadequate for imaging complex liquids. In fact, quite often reviewers of submitted manuscripts request cryo-EM micrographs to lend more support to assumptions suggested by authors. At the same time one still finds in the scientific literature electron micrographs that are clearly artifactual. Better availability and wide spread expertise of the cryo-EM methodologies should improve, if not solve, that problem.

## Acknowledgments

I thank a number of past and current graduate and undergraduate students of my group who have taken part in the development and application of cryo-EM in recent years: Ido Ben-Barak, Irina Davidovich,

Sharon Golan, Liron Issman, Tamar Kadosh, Olga Kleinerman, Na'ama Koifman, Lucy Liberman, Alona Makarsky, Maayan Nir, Liora Omer, Liat Oss-Ronen (postdoc), Maor Ronen, and Maya Schnabel. Some of the recent work has been done in close collaboration with my colleagues and friends at the Technion and other universities, and their group members: Volker Abetz (Hamburg University and the Helmholtz-Zentrum Geesthacht), Nicholas L. Abbot and David M. Lynn (University of Wisconsin), Benjamin Brenner and Anat Aharon (Technion), Simon Benita (Hebrew University of Jerusalem), Yachin Cohen (Technion), Daniela Goldfarb (Weizmann Institute), Heinz Hoffman (University of Bayreuth), James L. Lee (Ohio State University), Shlomo Magdassi (Hebrew University of Jerusalem), Maura Monduzzi and Sergio Murgia (University of Cagliari), Matteo Pasquali (Rice University), Lee R. Penn (University of Minnesota), Jacques Zakin (Ohio State University), and Raoul Zana (CNRS, Strasbourg). Special thanks go to the permanent members of my research group: Ellina Kesselman, Judith Schmidt, and Berta Shdemati. Recent financial support to the work has come from the United States — Israel Binational Science Foundation (BSF), the Israel Science Foundation (ISF), The European Union FP7, the Israel Ministry of Science and Technology (MOST), and the Dead Sea Works. The microscopy work has been performed at the Technion Laboratory for Electron Microscopy of Soft Matter, supported by the Technion Russell Berrie Nanotechnology Institute (RBNI), which has also provided the work with a Nevet research grant.

## References

[1] P. Echlin, R. Paden, B. Dronzek, R. Wayte, Proc. 3rd. Ann. Scanning Electron Microsc. Symp, 1970 (Chicago, IL).
[2] R.M. Glaeser, K.A. Taylor, J. Microsc. 112 (1978) 127–138.
[3] M. Adrian, J. Dubochet, J. Lepault, A.W. McDowall, Nature 308 (1984) 32–36.
[4] Y. Talmon, M. Adrian, J. Dubochet, J. Microsc. 141 (1986) 375–384.
[5] Y. Talmon, Ultramicroscopy 14 (1984) 305–316.
[6] J.R. Bellare, H.T. Davis, L.E. Scriven, Y. Talmon, J. Electron Microsc. Tech. 10 (1988) 87–111.
[7] L. Issman, Y. Talmon, J. Microsc. 246 (2012) 60–69.
[8] S. Ruthstein, J. Schmidt, E. Kesselman, Y. Talmon, D. Goldfarb, J. Am. Chem. Soc. 128 (2006) 3366–3374.
[9] D. Danino, R. Gupta, J. Satyavolu, Y. Talmon, J. Colloid Interface Sci. 249 (2002) 180–186.
[10] V.A. Davis, A.N.G. Parra-Vasquez, M.J. Green, P.K. Rai, N. Behabtu, V. Prieto, R.D. Booker, J. Schmidt, E. Kesselman, W. Zhou, H. Fan, W.W. Adams, R.H. Hauge, J.E. Fischer, Y. Cohen, Y. Talmon, R.E. Smalley, M. Pasquali, Nat. Nanotechnol. 4 (2009) 830–834.
[11] O. Kleinerman, A.N.G. Parra-Vasquez, M.J. Green, N. Behabtu, J. Schmidt, E. Kesselman, C.C. Young, Y. Cohen, M. Pasquali, Y. Talmon, J. Microsc. (2015) http://dx.doi.org/10.1111/jmi.12243 (in press).
[12] Y. Yan, H. Hoffmann, A. Makarsky, W. Richter, Y. Talmon, J. Phys. Chem. B 111 (2007) 6374–6382.
[13] I. Ben-Barak, Y. Talmon, Z. Phys. Chem. 226 (2012) 665–674.
[14] A. Bernheim-Groswasser, T. Tlusty, S.A. Safran, Y. Talmon, Langmuir 15 (1999) 5448–5453.
[15] B.W. Ninham, S.J. Chen, D.F. Evans, J. Phys. Chem. 88 (1984) 5855.
[16] S.J. Chen, D.F. Evans, B.W. Ninham, D.J. Mitchell, F.D. Blum, S.J. Pickup, J. Phys. Chem. 90 (1986) 842–847.
[17] L. Wolf, H. Hoffmann, T. Teshigawara, T. Okamoto, Y. Talmon, J. Phys. Chem. B 116 (2012) 2131–2137.
[18] M. Kahlweit, R. Strey, D. Haase, H. Kunieda, T. Schmeling, B. Faulhaber, M. Borkovec, H.F. Eicke, G. Busse, F. Eggers, T. Funck, H. Richmann, L. Magid, O. Soderman, P. Stilbs, J. Winkler, A. Dittrich, W. Jahn, J. Colloid Interface Sci. 118 (1987) 436–453.
[19] W. Jahn, R. Strey, J. Phys. Chem. 92 (1988) 2294–2301.
[20] J.L. Burns, Y. Cohen, Y. Talmon, J. Phys. Chem. 94 (1990) 5308–5312.
[21] L. Omer, S. Ruthstein, D. Goldfarb, Y. Talmon, J. Am. Chem. Soc. 131 (2009) 12466–12473.
[22] N. Koifman, M. Schnabel-Lubovsky, Y. Talmon, J. Phys. Chem. B 117 (2013) 9558–9567.
[23] N. Behabtu, J.R. Lomeda, M.J. Green, A. Higginbotham, A. Sinitskii, A.N.G. Parra-Vasquez, D.V. Kosynkin, J. Schmidt, E. Kesselman, Y. Cohen, Y. Talmon, J.M. Tour, M. Pasquali, Nat. Nanotechnol. 5 (2010) 406–411.
[24] N. Behabtu, C.C. Young, D.E. Tsentalovich, O. Kleinerman, X. Wang, A.W.K. Ma, E.A. Bengio, R.F. ter Waarbeek, J.J. de Jong, R.E. Hoogerwerf, S.B. Fairchild, J.B. Ferguson, B. Maruyama, J. Kono, Y. Talmon, Y. Cohen, M.J. Otto, M. Pasquali, Science 339 (2013) 182–186.
[25] P.J. Flory, Proc. R. Soc. Lond. A Math. Phys. Sci. 234 (1956) 73–89.
[26] L. Oss-Ronen, J. Schmidt, V. Abetz, A. Radulescu, Y. Cohen, Y. Talmon, Macromolecules 45 (2012) 9631–9642.
[27] Y. Talmon, J. Colloid Interface Sci. 93 (1983) 366–382.
[28] A. Wittemann, M. Drechsler, Y. Talmon, M. Ballauff, J. Am. Chem. Soc. 127 (2005) 688–9689.
[29] S. Attili-Qadri, N. Karra, A. Nemirovski, O. Schwob, Y. Talmon, T. Nassar, S. Benita, Proc. Natl. Acad. Sci. 110 (2013) 17498–17503.
[30] N. Arraud, R. Linares, S. Tan, C. Gounou, J.-M. Pasquet, S. Mornet, A.R. Brisson, J. Thromb. Haemost. 12 (2014) 614–627.
[31] L. Issman, B. Brenner, Y. Talmon, A. Aharon, PLoS ONE 8 (e83680) (2013) 1–9.
[32] Y. Talmon, Ber. Bunsenges. Phys. Chem. 100 (1996) 364–372.